XLIII CILAMCE
21-25, November, 2022
FOZ DO IGUAÇU - PR - BRAZIL

Dimensioning of sheet bending process trough ductile damage

Lucas de O. Barros[1], Ricardo N. Miranda[1], Caio C. A. Bílio[1], Caio R. A. de Lacerda[1], Paulo H. R. Brandão[1], Lucival Malcher[1]

[1]*Dept. of Mechanical Engineering, University of Brasilia*
Asa Norte, 70910-900, Brasilia/Federal District, Brazil
oliveira.barros@aluno.unb.br, ricardonm99@gmail.com, caiocesarabreu@hotmail.com, caio231098@gmail.com, pauloreisbrandao1998@gmail.com, malcher@unb.br

Abstract. This work seeks to dimension the sheet metal bending process through the control of ductile damage. For this, the material parameters of a 6101-T6 aluminum alloy are used. The process is simulated on a commercial finite element tool as an elastoplastic problem with ductile damage. Parameters such as sheet thickness and geometry of forming tools are evaluated. Thus, possible problems associated with the process are analyzed, such as cracks in the bending regions, fractures and deformations. Three sheet thicknesses are evaluated, more specifically 1, 2 and 3 mm. For the 3 mm sheet, a new geometry of the forming tool was proposed in order to smooth the entire process. Three parts were modeled for analysis: two parts for forming the sheet, called tools "A" and "B", and the sheet. Tool “A” works like a punch, tool “B” works like a mold. The problem was modeled considering plane strain state. The tools used for the sheet bending process are modeled as rigid bodies, whereas the sheet is modeled as a deformable solid.

Keywords: Sheet metal bending process, 6101-T6 aluminum, ductile damage.

1 Introduction

The sheet bending process is a common and vital process in industries and widely used by companies operating in the steel market. Bending consists in generating a deformation along an axis, in order to change the geometry of the part. It is similar to other metal forming processes, however sheet bending changes the shape of the workpiece while the volume of the material remains the same [1],[2],[3].

Thus, in sheet metal bending, according to Filho [4], efforts are applied in two opposite directions to cause bending and plastic deformation, with the objective of changing the flat shape into two competing surfaces, at an angle, with radius of agreement at the junction. Chiaverini [5] emphasizes that, in bending, it is sought to avoid any dimensional change, especially the thickness of the sheet, as well as the presence of sharp corners.

In the region where the two surfaces meet through bending, the conformation efforts are concentrated, so that, on the outside, there are tensile forces, while, on the inside, there are compression forces. As there are opposite directions of force between the inner and outer faces, at an intermediate point along the line perpendicular to the sheet, which is the neutral point, the stresses are equal to zero. By joining all the neutral points along the sheet, the neutral line is obtained. It is assumed that the neutral line length remains the same before and after forming [6]. According to Choudhry [7] and Barbosa [8] the other lines along the sheet do not maintain the same initial lengths, so the neutral line is a reference for the development of the bent part. Besides, according to Filho [4], the potential fracture occurs on the outside, if the stresses exceed the tensile strength limit of the material, and the possible wrinkling on the inside is due to the action of compression efforts, especially in sheets with smaller thickness.

The bending angle in the former operation must be greater than a determined value, due to the occurrence of elastic recovery. This phenomenon becomes more critical as the material yield strength, sheet thickness and bending angle increase and as the bending radius decreases. Thus, it is usual to apply a greater bending force in order to obtain the expected result after elastic recovery [1].

In particular, press bending can be divided into two steps: the correct positioning of the specimen and press activation until bending is complete. Therefore, this work aims to evaluate sheet bending, through simulations in the ABAQUS software of sheets with thicknesses of 1, 2 and 3 mm. For that, a mesh convergence study and analysis of the results are carried out.

2 Materials and Methods

The modeling of the problem was defined as explicit, that is, the behavior of the system is verified at each defined time step. The modeling involved 3 parts in two dimensions, following the same logic for each configuration analyzed. The first part is a punching tool ("A") and the second part is a mold tool ("B"), both modeled as rigid bodies. The third part is the sheet to be bent, which is modeled as a deformable body. The configuration of the parts was the tool "A" on top, the tool "B" on the bottom and the sheet in between. This arrangement was made in such a way that by fixing the movement in all degrees of freedom of tool "B", a displacement of 15 mm in the "y" direction would be applied to tool "A", thus perfectly bending the sheet over the mold "B". The process is considered as plane strain state. Fig. 1 shows the representation of the exploded view of the model.

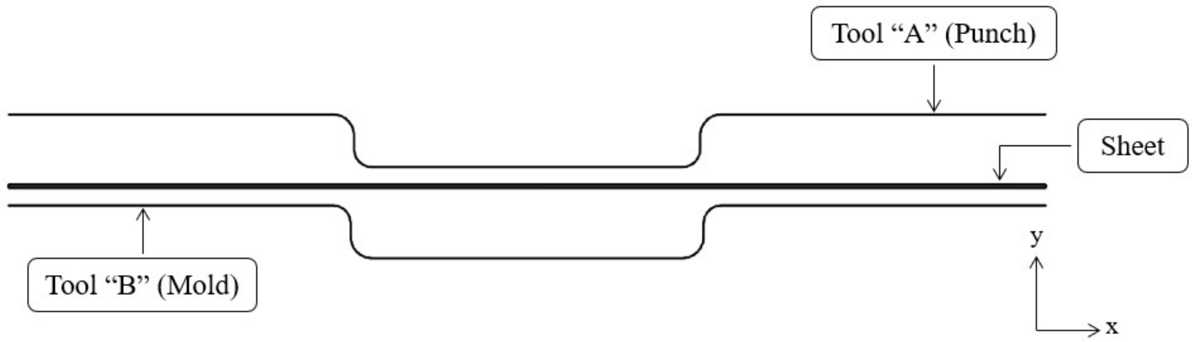

Figure 1: Exploded view of modeling

In the first configuration, the plate is initially 1 mm thick and 300 mm long, as shown in Fig. 2. The fillets were made in order to smooth the stress concentration and bend the sheet rather than fracturing it.

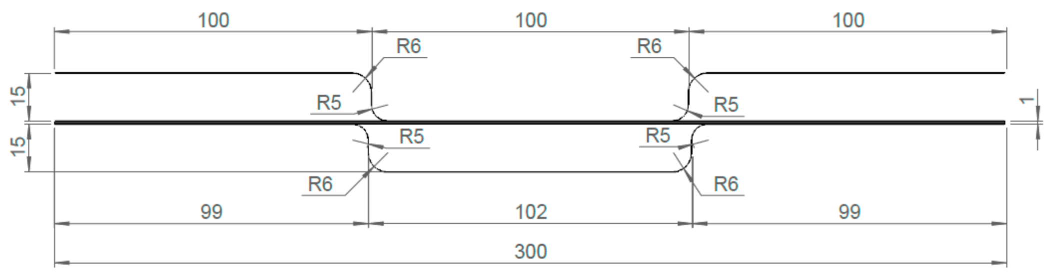

Figure 2. 1 mm thick sheet

In the second configuration, the plate is 2 mm thick and 300 mm long, as shown in Fig. 3.

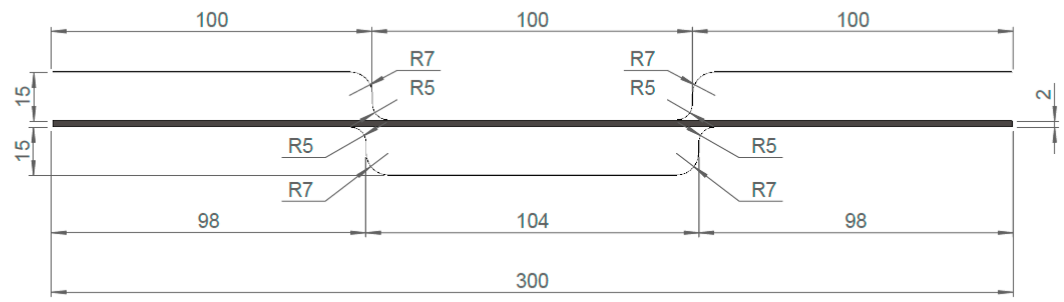

Figure 3. 2 mm thick sheet

In the third configuration, on the other hand, a 3 mm thick and 300 mm long plate is adopted, as shown in Fig. 4.

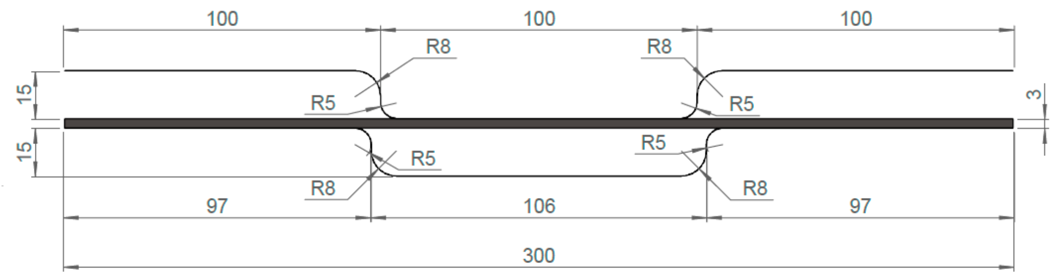

Figure 4. 3 mm thick sheet

Finally, in the last configuration, the 3 mm thick and 300 mm long plate is adopted, however with a different geometry proposal for the tools. In Fig. 5, this fourth configuration is detailed.

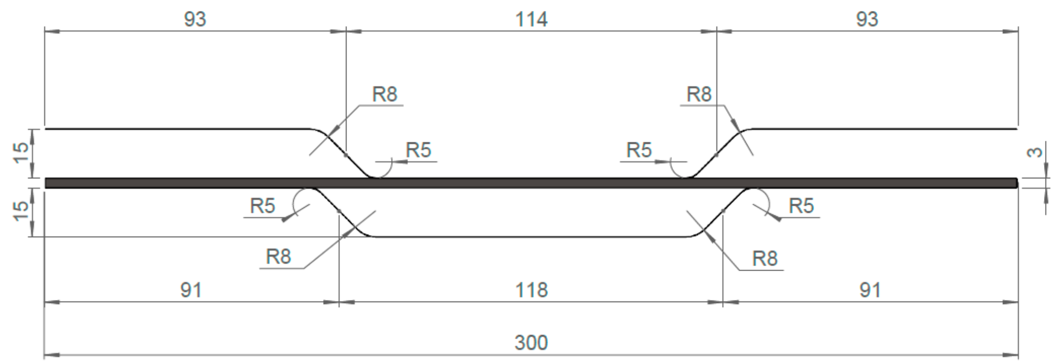

Figure 5. Thickness of 3 mm, another geometry proposal for the tools

To obtain the properties of aluminum 6101, experimental tests were carried out using an MTS 810 uniaxial testing machine with an axial load capacity of 100 kN. Two models of specimens were manufactured: smooth and notched. Smooth bodies have a circular cross section, while notched bodies have a square cross section. The circular section bodies were subjected to tensile tests, while the square section bodies were subjected to pure shear and combined tensile and shear loads [9], [10]. In Tab. 1, the elastic properties stipulated for Aluminum 6101 are shown.

Table 1: Elastic proprieties of Aluminum 6101

Proprieties	Nomenclature	Value
Elasticity Module	E	70.000 GPa
Poisson's Coefficient	υ	0.3
Density	d	0.0027 g/mm^3

In Tab. 2, the plastic properties of the material are shown as various values of yield stress and correspondent plastic deformation.

Table 2: Plastic proprieties of Aluminum 6101

Yield Stress (MPa)	Plastic Deformation
96	0
110.862939	0.01
124.104035	0.02
135.908122	0.03
146.438970	0.04
155.841683	0.05
164.244838	0.06
171.762343	0.07
178.495134	0.08
184.532642	0.09
189.954106	0.10
210.016430	0.15
222.406358	0.20
230.606585	0.25
236.518924	0.30
245.162664	0.40
252.175574	0.50
258.702203	0.60
265.083819	0.70
271.422192	0.80
277.747672	0.90
284.069306	1.00
290.389793	1.10
296.709938	1.20
303.029982	1.30
309.349994	1.40
315.669998	1.50

Tab. 3 shows the properties related to ductile damage and damage evolution of the material.

Table 3: Ductile damage properties

Fracture Strain	Stress Triaxiality	Stain Rate	Displacement at fracture
0.15	0	0	0.03

Therefore, the step of the simulation is defined using the "Nlgeom: On" function, which includes the non-linear effects for large deformations. Afterwards, the interaction properties are defined as normal and tangential behaviors. Finally, before creating the mesh and carrying out the simulations, the contacts between each tool and the sheet are then defined, with the tools as "master" surfaces and the sheet as "slave" surface, the main purpose of this configuration is to analyze the part of interest, which is the sheet.

3 Results and Analysis

In the analysis of the results, initially, a mesh convergence study is carried out. The importance of this assessment is due to the fact that the results vary according to the level of discretization, element type and other parameters related to the finite elements. Therefore, the goal is to find the thickest mesh as possible which allows the stabilization of one or more parameters.

Thus, through the physical data of the problem and modeling in the computer program ABAQUS, different quantities and types of elements are combined in order to observe the effects on von Mises stress. The graph in Fig. 6 presents the results.

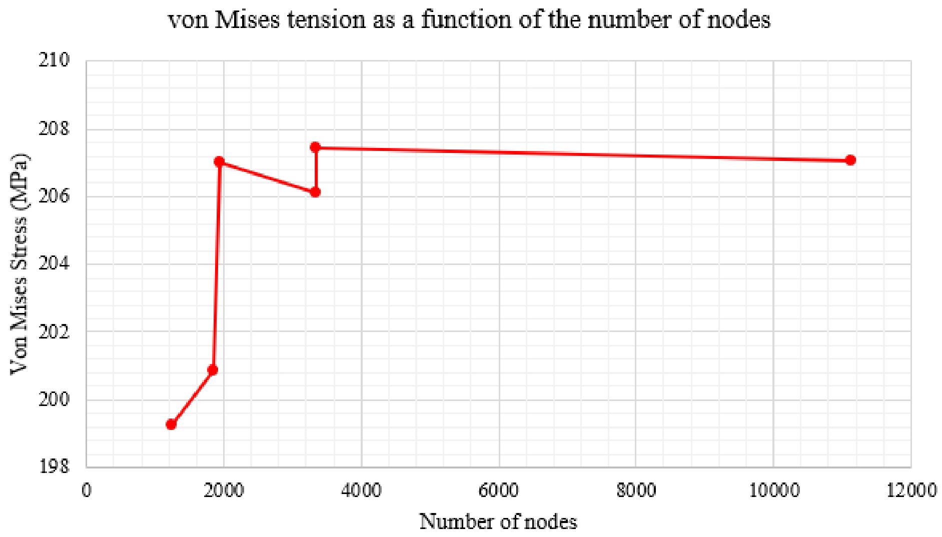

Figure 6. Graph of von Mises tension as a function of the number of nodes.

According to Fig. 6, in view of the objective of determining the thickest mesh as possible, the chosen mesh is the one described in Tab. 5.

Table 4: Selected mesh information

Tool 1 (Punch)		Tool 2 (Mold)		Sheet	
Element	N° of nodes	Element	N° of nodes	Element	N° of nodes
Rigid, linear, two-dimensional, with two nodes	164	Rigid, linear, two-dimensional, with two nodes	164	Plane stress, quadrilateral, bilinear, with four nodes and reduced integration	3005

The mesh with 3333 nodes in the graph in Fig. 6, whose characteristics are detailed in Tab. 5, is selected because it reached a satisfactory level of stabilization of the von Mises stress values. Furthermore, this mesh corresponds to the global element size of 0.5 mm for the plate, which also guarantees a suitable mesh for the sheet with a thickness of 1 mm.

In Fig. 7 a) and Fig. 7 b), the results for the bending of a 1 mm sheet are shown. The maximum values of Mises tension are approximately 180.60 MPa and the accumulated deformation 0.10. The images show certain regions of stress concentration; however, no crack initiation or fracture is observed in the sheet.

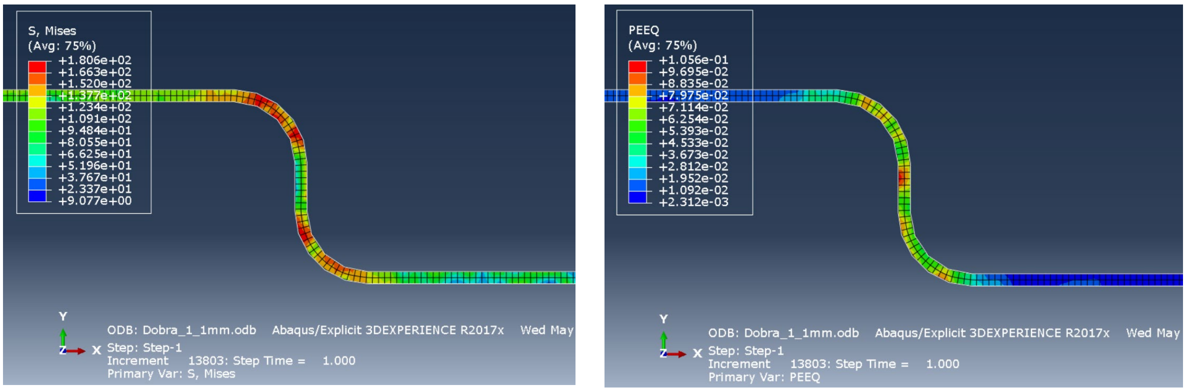

a) b)

Figure 7. a) Mises stresses in the regions of stress concentration, for a sheet with a thickness of 1 mm. b) Accumulated plastic deformation in the regions of stress concentration, for a sheet with a thickness of 1 mm.

To conduct a further study of the sheet bending process, other simulations were made in the same configuration, but using sheet thicknesses of 2 and 3 mm. Fig. 8 a) and Fig. 8 b) represent the results of the simulation with the 2 mm sheet. It can be observed that some elements were deleted, which implies that the failure criterion was triggered so that under the conditions established for the problem, a sheet made of the chosen material would not support the tensions and would consequently fracture.

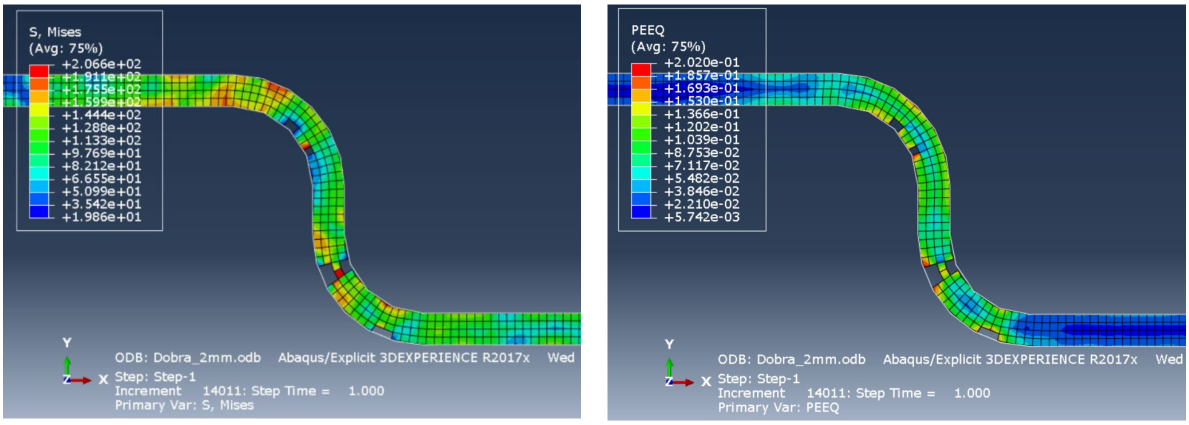

a) b)

Figure 8. a) Mises stresses in the regions of stress concentration, for a sheet with a thickness of 2 mm. b) Accumulated plastic deformation in the regions of stress concentration, for a sheet with a thickness of 2 mm.

Fig. 9 a) and Fig. 9 b) demonstrate the simulation results with the 3 mm sheet. It is possible to observe that there is a fracture during the sheet bending process. It is also clear that the values of stress and accumulated plastic deformation are relatively higher when compared to thinner sheets.

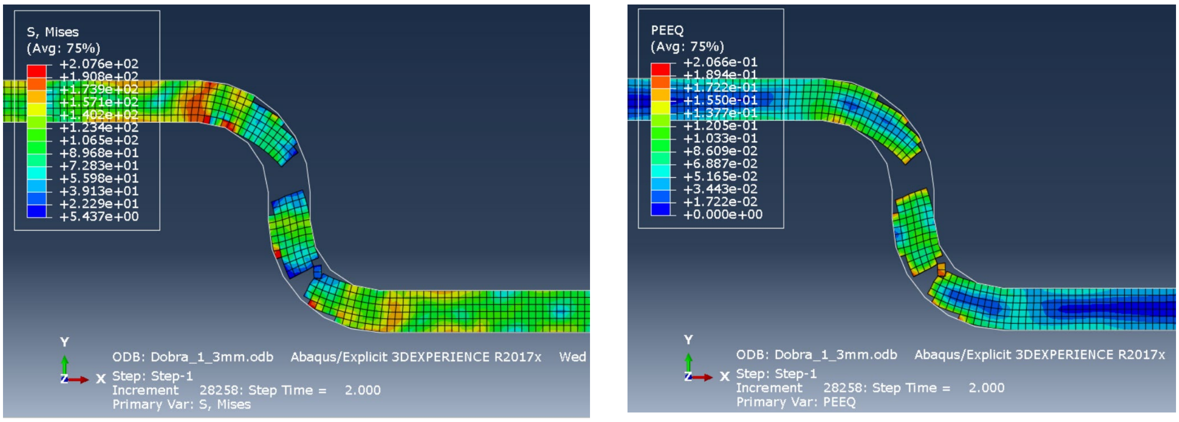

a) b)

Figure 9. a) Mises stresses in the regions of stress concentration, for a sheet with a thickness of 2 mm. b) Accumulated plastic deformation in the regions of stress concentration, for a sheet with a thickness of 2 mm.

Finally, a new configuration was proposed for the 3 mm sheet, in order to provide a smoother bending so that the sheet did not fracture, as shown in Fig. 10. The tilt angle of the fold was changed to 45º. Fig. 11 a) and Fig. 11 b) present the results obtained from the simulation.

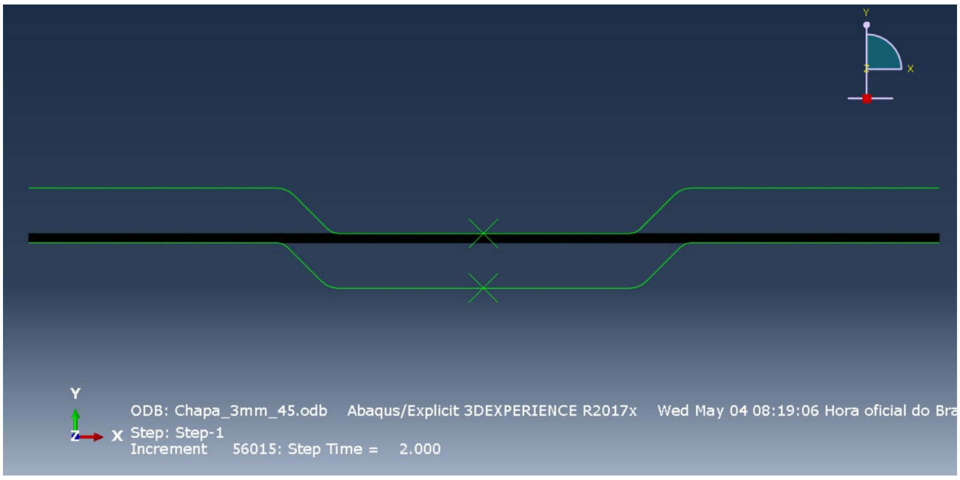

Figure 10. Assembly of the problem of the 3 mm sheet with 45º inclination

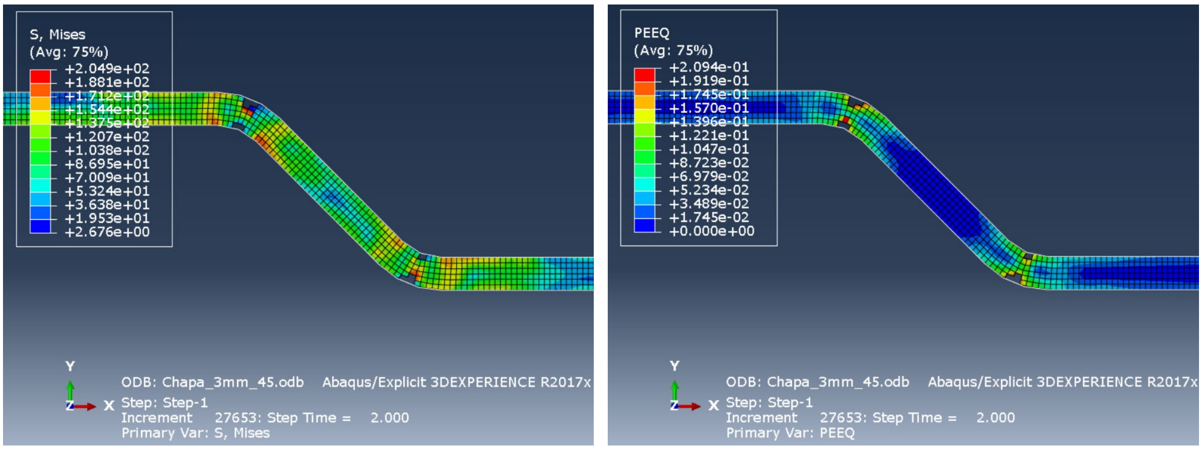

a) b)

Figure 11. a) Mises stresses in the regions of stress concentration, for a 3 mm thick sheet with 45° inclination. b) Accumulated plastic deformation in the regions of stress concentration, for a 3 mm thick sheet with 45º inclination.

Despite the attempt to prevent the plate from fracturing, the tensions were still high enough to activate the failure criterion in a significant number of elements, so the sheet again started to fracture. Yet, as opposed to what happened using the tools at an angle of 90 °, the total breakage of the sheet did not occur for this last simulation.

4 Conclusions

According to the results obtained by the simulation, it was possible to observe the influence of the sheet thickness on whether or not cracks and fractures would appear during the bending process. In this sense, it is remarkable that the greater the thickness of the plate, the greater the likelihood of its fracture, given the increase of its rigidity and, consequently, the greater the deformations necessary to ensure its correct accommodation in the tool. As seen in the previous section, for the plates with thickness of 1 mmm, there is no complication of cracks and fractures during the bending process, and the accumulated plastic deformation levels are relatively lower when compared to the sheet with larger thicknesses. As the thickness increases, cracks and fractures start to emerge. In 2 mm thickness simulations, there is the emergence of cracks during the folding process, whereas with a thickness of 3 mm, there is fracture of the sheet.

On the other hand, the influence of the conformation angle on the bending process was also observed. It was observed that, using a tool with an inclination of 45°, lower stresses were obtained when compared to with a 90° contour, as shown in Fig. 9 a) and Fig. 11 a). The new part geometry also shows that the 3 mm sheet did not fracture during the entire forming process, as opposed the tool angle of 90°. Thus, the reduction in stresses during the bending process directly influences the deformation supported by the sheet and its ability to conform without cracking.

Acknowledgements. The authors thank the University of Brasília for their support, CAPES and CNPQ.

Authorship statement. The authors hereby confirm that they are the sole liable persons responsible for the authorship of this work, and that all material that has been herein included as part of the present paper is either the property (and authorship) of the authors, or has the permission of the owners to be included here.

References

[1] S. K. Panthi, N. Ramakrishnan, K. K. Pathak, and J. S. Chouhan, "An analysis of springback in sheet metal bending using finite element method (FEM)," *Journal of Materials Processing Technology*, vol. 186, no. 1–3, pp. 120–124, May 2007, doi: 10.1016/j.jmatprotec.2006.12.026.
[2] J. R. Cho, S. J. Moon, Y. H. Moon, and S. S. Kang, "Finite element investigation on spring-back characteristics in sheet metal U-bending process," *Journal of Materials Processing Technology*, vol. 141, no. 1, pp. 109–116, Oct. 2003, doi: 10.1016/S0924-0136(03)00163-8.
[3] V. Esat, H. Darendeliler, and M. I. Gokler, "Finite element analysis of springback in bending of aluminium sheets," *Materials and Design*, vol. 23, pp. 223–229, 2002.
[4] B. Filho, I. B. Silva, F. G. Batalha, and S. T. Button, *CONFORMAÇÃO PLÁSTICA DOS METAIS*, 1st ed. São Paulo, 2011.
[5] V. Chiaverini, *Tecnologia Mecânica*, 2nd ed., vol. II. São Paulo: McGraw-Hill Ltda, 1986.
[6] E. Safronov and A. Nosko, "Analysis of Linear Dimension Accuracy of Sheet Metal Bending," *MATEC Web of Conferences*, vol. 346, p. 01007, Oct. 2021, doi: 10.1051/matecconf/202134601007.
[7] S. Choudhry and J. K. Lee, "Dynamic plane-strain finite element simulation of industrial sheet-metal forming processes," *Int. J. Mech. Sci*, vol. 36, no. 3, pp. 189–207, 1994.
[8] G. M. Barbosa, "Processo de dobramento de chapas metálicas," *Exacta*, vol. 7, no. 1, pp. 109–120, 2009.
[9] L. Malcher *et al.*, "Experimental program and numerical assessment for determination of stress triaxiality and J3 effects on AA6101-T4," *Theoretical and Applied Fracture Mechanics*, vol. 106, Apr. 2020, doi: 10.1016/j.tafmec.2020.102476.
[10] V. A. M. Rodrigues, L. L. D. Morales, and L. Malcher, "Mechanical behavior of 6101 Aluminum alloy," *Cilamce XLI*, Nov. 2020.